2-17-2014

Electrocatalytic CO2 reduction by M(bpy-R)(CO)4 (M = Mo, W; R = H, tBu) complexes. Electrochemical, spectroscopic, and computational studies and comparison with group 7 catalysts

Melissa L. Clark

Kyle A. Grice

Curtis E. Moore

Arnold L. Rheingold

Clifford P. Kubiak

Recommended Citation
Chem. Sci., 2014,5, 1894-1900

Chemical Science

EDGE ARTICLE

View Article Online
View Journal | View Issue

Cite this: *Chem. Sci.*, 2014, **5**, 1894

Electrocatalytic CO_2 reduction by M(bpy-R)(CO)$_4$ (M = Mo, W; R = H, *t*Bu) complexes. Electrochemical, spectroscopic, and computational studies and comparison with group 7 catalysts†

Melissa L. Clark,‡ Kyle A. Grice,‡§ Curtis E. Moore, Arnold L. Rheingold and Clifford P. Kubiak*

Received 17th December 2013
Accepted 14th February 2014

DOI: 10.1039/c3sc53470g

www.rsc.org/chemicalscience

The tetracarbonyl molybdenum and tungsten complexes of 2,2′-bipyridine and 4,4′-di-*tert*-butyl-2,2′-bipyridine (M(bpy-R)(CO)$_4$; R = H, M = Mo (**1**), W (**2**); R = *t*Bu, M = Mo (**3**), W (**4**)) are found to be active electrocatalysts for the reduction of CO_2. The crystal structures of M(bpy-*t*Bu)(CO)$_4$ (M = Mo (**3**), W (**4**)), the singly reduced complex [W(bpy)(CO)$_4$][K(18-crown-6] (**5**) and the doubly reduced complex [W(bpy-*t*Bu)(CO)$_3$][K(18-crown-6)]$_2$ (**6**) are reported. DFT calculations have been used to characterize the reduced species from the reduction of W(bpy-*t*Bu)(CO)$_4$ (**4**). These compounds represent rare examples of group 6 electrocatalysts for CO_2 reduction, and comparisons are made with the related group 7 complexes that have been studied extensively for CO_2 reduction.

Introduction

The electrocatalytic reduction of CO_2 to value-added products and fuels is an area that has seen significant progress over the last several decades.[1–5] In particular, the use of homogeneous electrocatalysts is an attractive approach because they can be studied with a variety of techniques and modified *via* synthesis to affect reactivity. Previous work from our group focused on the study of complexes of the type M(bpy-R)(CO)$_3$X (M = Re, Mn; R = H, *t*Bu, *etc.*), based on the 2,2′-bipyridine system originally reported by Lehn.[6] Our more recent studies have shown that the 4,4′-di-*tert*-butyl-2,2′-bipyridine (bpy-*t*Bu) ligand is effective in increasing the activity of rhenium-based CO_2 reduction catalysts compared to the complexes of their 2,2′-bipyridine counterparts.[7–9]

Many homogeneous electrocatalysts for CO_2 reduction are based on expensive and rare metals such as Ru and Re. The cost of these metals makes it difficult to envision their use in large-scale deployment of systems for the synthesis of renewable chemicals and fuels from CO_2. Significant progress has been made towards developing electrocatalysts based on more abundant metals (for example: Mn,[10,11] Ni,[12] Fe,[13,14] and Cu[15]). Notably, there are very few reports of electrocatalytic CO_2 reduction catalysts based on complexes of group 6 metals (Cr, Mo, W),[16,17] even though this group contains the metals commonly found in the active sites of formate dehydrogenase (FDH) enzymes, which interconvert CO_2 and formate.[18] Aerobic bacteria also utilize molybdenum in the active site of carbon monoxide dehydrogenase (CODH) enzymes that are capable of oxidizing CO to CO_2.[19]

Stoichiometric reactions of dianionic Cr, Mo and W pentacarbonyl complexes with CO_2 lead to the formation of coordinated CO (Scheme 1),[20] and there are other examples of stoichiometric CO_2 reduction at homogeneous group 6 metal

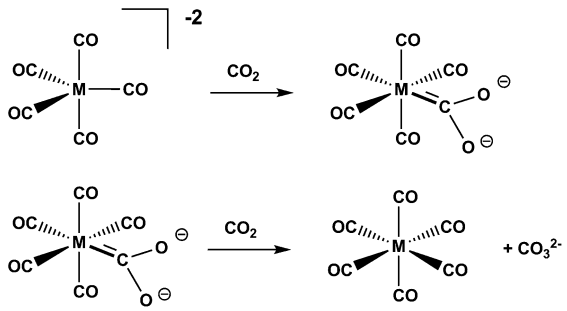

Scheme 1 Reactions of group 6 dianions with CO_2 (M = Cr, Mo, W).[20]

Department of Chemistry and Biochemistry, University of California, San Diego, 9500 Gilman Drive MC 0358, La Jolla, California 92093, USA. E-mail: ckubiak@ucsd.edu; Fax: +1 858 534 5383; Tel: +1 858 822 2665

† Electronic supplementary information (ESI) available: Synthesis and experimental details, additional electrochemistry results, additional FT-IR data, crystallographic data tables, and DFT geometry optimized coordinates. CCDC 967672–967675. For ESI and crystallographic data in CIF or other electronic format see DOI: 10.1039/c3sc53470g

‡ These authors had equal contribution.

§ Current address: Department of Chemistry, DePaul University, 1110 W. Belden Ave, Chicago, IL, 60614, USA.

complexes.[21–23] The coupling of CO_2 with olefins,[24] as well as hydrogenation of CO_2 to formic acid[25] or alkyl formates[26] have been observed at group 6 complexes. Given the precedent for CO_2 reactivity with group 6 complexes, we were curious to see if 2,2′-bipyridine complexes of these group 6 metals could be used as *electrocatalysts* for the reduction of CO_2 to produce value-added products such as CO.

The spectroscopic, photochemical, and electrochemical properties of group 6 complexes of the type $M(L)(CO)_4$ (M = Cr, Mo, W, L = diimine ligand) are well known.[27] It has been proposed that the reduction of these metal complexes by two electrons leads to the loss of a CO ligand and generation of a five-coordinate $[M(L)(CO)_3]^{2-}$ species,[27,28] although spectroscopic characterization of such species has not been reported. We note the parallel between this postulated $[M(L)(CO)_3]^{2-}$ species and the dianionic $[M(CO)_5]^{2-}$ complexes reported by Cooper and co-workers to react with CO_2 to form $M(CO)_6$,[20] thus reducing CO_2 to CO. The group 6 dianionic $[M(bpy\text{-}R)(CO)_3]^{2-}$ complexes are also formally isoelectronic to the five-coordinate $[Re(bpy\text{-}tBu)(CO)_3]^-$ and $[Mn(bpy\text{-}tBu)(CO)_3]^-$ anions, the critical intermediates that react with CO_2 in electrocatalytic reduction of CO_2 by $Re(bpy\text{-}tBu)(CO)_3X$ and $Mn(bpy\text{-}tBu)(CO)_3X$.[11]

Herein we report electrochemical studies of the group 6 complexes $M(bpy\text{-}R)(CO)_4$ (R = H, M = Mo (**1**), W (**2**); R = *t*Bu, M = Mo (**3**), W(**4**)). We find that these complexes are electrocatalysts for the reduction of CO_2. Particular focus is placed on complex **4**, as it is isoelectronic with previously published highly active rhenium and manganese systems. NMR spectroscopy, X-ray crystallography, and Density Functional Theory (DFT) studies are also used to examine the species relevant to catalytic CO_2 reduction. The comparisons between the group 6 and group 7 complexes contribute to a clearer understanding of the specific characteristics that lead to more active CO_2 reduction catalysts.

Results and discussion

Synthesis and characterization

The known complexes $M(bpy\text{-}R)(CO)_4$ (M = W, Mo; R = H, *t*Bu, **1–4**, Fig. 1), were synthesized similar to literature procedures.[29] These complexes were isolated as bright orange-red (M = Mo) or dark red (M = W) air-stable solids. Although complex **4** has been mentioned in the literature,[30–32] its ^1H and ^{13}C NMR spectra had not been previously reported, and this data is included in the ESI.† The FT-IR spectra of these complexes display the standard four-signal pattern ($2A_1$, B_1, and B_2) in the ν(CO) region (1700–2100 cm^{-1}, Fig. S1 in the ESI†) for tetracarbonyl complexes of this type with values that are in agreement with the literature (Table S1 in the ESI†).[33,34] The addition of the *t*Bu groups increases the solubility of **3** and **4** in organic solvents compared to **1** and **2**.

In order to compare with the reported X-ray structures of $M(bpy)(CO)_4$ (M = Mo (**1**),[35] W (**2**)[36,37]), X-ray quality crystals were grown of the *tert*-butyl derivatives $M(bpy\text{-}tBu)(CO)_4$ (M = Mo (**3**), W (**4**); see Fig. 2) by vapor diffusion of pentane into concentrated toluene solutions of the complexes. The molecular geometries of **3** and **4** are similar to the corresponding complexes with the parent bipyridine ligand (**1** and **2**), with slightly shorter M–N bonds (Table S2†), indicating slightly stronger donation from the *tert*-butyl ligand and slightly stronger back donation to the M–CO groups. This is also observed in the FT-IR data for complexes **1–4**, in which the ν(CO) frequencies are shifted to lower wavenumbers on the *t*Bu-substituted complexes compared to the parent complexes. The C–C bond lengths between the two pyridyl rings (C9–C10) for all of the complexes are consistent with a neutral bipyridine ligand.[38]

A search of the Cambridge Crystallographic Database did not yield any other tetracarbonyl tungsten or molybdenum complexes with 4,4′-disubstituted bipyridine ligands.[39] However, a comparison of the structures of **1–4** with previously reported isoelectronic $[Re(bpy\text{-}R)(CO)_4](OTf)$ complexes reveals interesting similarities and differences. The bending of the axial CO ligands away from the bipyridine ligands in complexes **1–4** (as seen in the M–C1–O1 and M–C4–O4 angles of *ca.* 171–172°) is a common feature of group 6 tetracarbonyl complexes, and

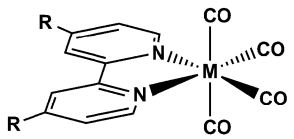

(**1**) M = Mo, R = H
(**2**) M = W, R = H
(**3**) M = Mo, R = *t*Bu
(**4**) M = W, R = *t*Bu

Fig. 1 Tetracarbonyl complexes of molybdenum and tungsten examined in this work.

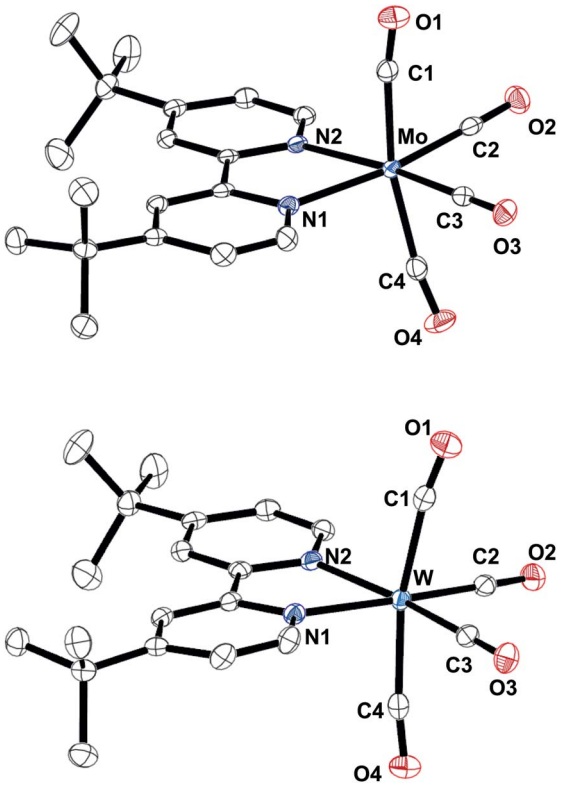

Fig. 2 Molecular structures of **3** (top) and **4** (bottom), with ellipsoids shown at 50% probability and hydrogen atoms excluded for clarity. Selected bond lengths and angles are listed in Table S2 in the ESI†.

has been explained in terms of back donation from a π* orbital on the bidentate diimine ligand.[40] This structural deviation of the metal carbonyls from linearity is also apparent in the structure of the d^6 [Re(bpy-R)(CO)$_4$](OTf) complexes (R = H, *t*Bu).[41,42] Notably, complex **4** has significantly longer C–O bond lengths compared to [Re(bpy-*t*Bu)(CO)$_4$](OTf), which is evidence of stronger back donation from the tungsten metal center. This is also reflected in the FT-IR spectra of **4** and the corresponding rhenium complex. They have similar patterns for the ν(CO) stretches in their FTIR spectra, but the stretches for the tungsten complex **4** are 116–138 cm^{-1} lower in energy than the rhenium complex in acetonitrile.

Electrochemical studies

The cyclic voltammograms of complexes **1–4** in acetonitrile are very similar, displaying one reversible reduction at *ca.* −1.6 V *vs.* SCE followed by an irreversible reduction at *ca.* −2.1 V *vs.* SCE (voltammogram for **1** shown in Fig. 3, reduction potentials for **1–4** are listed in Table 1 and voltammograms of **2–4** are shown in Fig. S2†). This data is similar to previously reported electrochemistry for **1** and **2** that was obtained in THF,[43,44] acetonitrile (1st reduction only),[45] and dimethoxyethane.[46,47] The first reduction of **3** has also been reported in multiple solvents.[48] The first reduction of these complexes is primarily localized on the bipyridyl ligand, forming stable 19-electron [M(bpy-R)(CO)$_4$]$^{\bullet-}$ species that have been previously characterized for the parent bipyridine complexes **1** and **2** by FT-IR,[46] UV-Vis,[28] and EPR spectroscopies.[28,49]

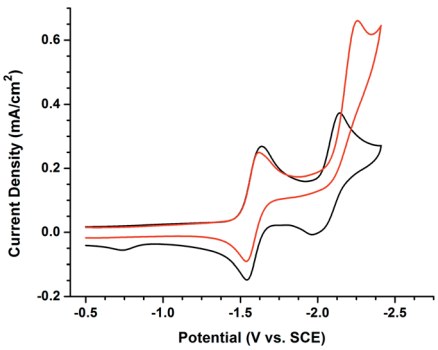

Fig. 3 Representative cyclic voltammogram of **1** at a scan rate of 100 mV s^{-1} under N_2 (black line) and CO_2 (red). Conditions: 1 mm diameter glassy carbon working electrode, platinum wire counter electrode, Ag/AgCl reference, decamethylferrocene (FeCp*$_2$) internal reference, 1 mM **1**, 0.1 M tetrabutylammonium hexafluorophosphate (TBAPF$_6$), room temperature. Complexes **2**, **3**, and **4** exhibit similar behavior (see ESI†).

Table 1 Reduction potentials *vs.* SCE for complexes **1–4**. All complexes were studied under the same conditions as stated for **1**

Complex	$E_{1/2}$ (V)	2nd[a] (V)
1	−1.58	−2.14
2	−1.49	−2.08
3	−1.66	−2.20
4	−1.58	−2.15

[a] Irreversible, reported as the location of the peak of the irreversible wave *vs.* SCE during the reductive sweep in the cyclic voltammogram at 100 mV s^{-1}.

Table 2 Comparison of the catalytic activity of complexes **1–4** to relevant group 7 complexes[11]

Complex	i_{cat}/i_p	TOF[a] (s^{-1})
Mo(bpy)(CO)$_4$ (**1**)	2.3	1.0
W(bpy)(CO)$_4$ (**2**)	3.4	2.2
Mo(bpy-*t*Bu)(CO)$_4$ (**3**)	3.1	1.9
W(bpy-*t*Bu)(CO)$_4$ (**4**)	3.9	2.9
[Re(bpy-*t*Bu)(CO)$_3$(CH$_3$CN)](OTf)[b]	3.3	2.1
Mn(bpy-tBu)(CO)$_3$Br[b]	1.0	0.0
[Re(bpy-*t*Bu)(CO)$_3$(CH$_3$CN)](OTf)[c]	54	570
Mn(bpy-tBu)(CO)$_3$Br[d]	42	340

[a] TOF for **1–4** obtained using method described by Smieja *et al.*[11] [b] Activity under similar conditions to those used for **1–4**. [c] 1.4 M 2,2,2-trifluoroethanol (TFE) added. [d] 1.6 M TFE added.

When acetonitrile solutions containing complexes **1–4** are exposed to a CO_2 atmosphere, the first reduction in the cyclic voltammograms is similar to the reduction under inert atmosphere. However, at the second reduction potential, a current increase is observed (i_{cat}/i_p = 2.3, 3.4, 3.1, and 3.9 for **1**, **2**, **3**, and **4**, respectively, Fig. 3), which is attributed to catalytic reduction of CO_2. These current enhancements occur at potentials that are similar to the peak potential of CO_2 reduction by Re(bpy-*t*Bu)(CO)$_3$Cl (−2.1 V *vs.* SCE).[7] The i_{cat}/i_p and the corresponding turnover frequencies (TOF, Table 2) show that the tungsten complexes are more active than the molybdenum complexes, and the *tert*-butyl groups enhance the activity for both metals. Complex **4** was selected for further study as it was the most active catalyst based on cyclic voltammetry (i_{cat}/i_p of 3.9), but more importantly because it is isoelectronic with the well-studied *fac*-Re(bpy-tBu)(CO)$_3$X species so that the most appropriate comparison can be made.

Scan-rate dependence studies for complex **4** (Fig. S3 in the ESI†) show that the second reduction remains irreversible even at high scan rates (*ca.* 10 V s^{-1}). The irreversibility of the second reduction indicates that a chemical reaction occurs following this reduction. This can be postulated as a loss of one CO ligand, although there is only brief mention of this in the literature, and full characterization for the dianions has not been previously reported.[27,28] The small oxidation wave observed at *ca.* −700 mV only appears after the second reduction is reached.

Controlled potential electrolysis

In order to study the catalytic reduction of CO_2, controlled potential electrolysis experiments were carried out with complex **4**. Care was taken to separate the counter electrode from the solution with a glass tube packed with a plug of glass wool during bulk electrolysis, because it has been shown that electrochemical oxidation of group 6 M(L)(CO)$_4$ complexes leads to the liberation of CO.[34] Bulk electrochemical reduction at −2.3 V under a CO_2 atmosphere led to formation of CO with a

109 ± 7% faradaic efficiency, as detected by gas chromatography (Fig. S4†). Carbon monoxide was also observed by gas chromatography when the same experiment was performed under inert atmosphere, due to the loss of a carbonyl ligand that occurs after the second reduction. The current density under CO_2 initially decreased after the start of the bulk electrolysis but stabilized at 0.66 mA cm^{-2}, whereas under N_2 it stabilized at 0.44 mA cm^{-2} (Fig. S5†). This verifies the catalytic activity observed in the cyclic voltammograms, and also indicates that the catalyst is highly selective for CO formation. There was no evidence of carbonate, formate, or other CO_2-derived products by NMR or FT-IR measurements of complex **4**, and therefore the reaction is likely of the form $CO_2 + 2e^- + 2H^+ \rightarrow CO + H_2O$, similar to the group 7 catalysts. The catalytic activity was observed to be stable over the course of several hours (Fig. S6†), indicating that the compound remains active over time. Hydrogen was observed only in small quantities (less than 3% faradaic efficiency).

Chemical reduction and characterization of the reduced species

Crystallographic characterization of the mono or di-reduced forms of M(bpy-R)$(CO)_4$ have not been reported, nor have the di-reduced species been characterized by spectroscopy. While the oxygen and proton sensitivity of these highly reduced forms makes isolation challenging, the anions and dianions of **2** and **4** were produced in yields of 40–70% and characterized by FT-IR and NMR (ESI†). After many attempts, crystal structures of the anion $[W(bpy)(CO)_4]^-$ (**5**) and dianion $[W(bpy\text{-}t\text{Bu})(CO)_3]^{2-}$ (**6**) were obtained. Addition of 1 equivalent of KC_8 to a solution of **2** and 18-crown-6 in THF led to the formation of a dark orange solution of the new species **5**. Vapor diffusion of pentane into a solution of **5** in THF led to black-orange crystals suitable for X-ray diffraction. Consistent with analogous anionic complexes,[7,8,11] the anionic tungsten complex crystallizes with the potassium cation enclosed in the crown ether, seen in Fig. 4. The potassium is both associated with an axial carbonyl (K–O bond length of 2.813(3) Å) and a THF solvent molecule. The bond length alteration in the 2,2′-bipyridine ring of **5** is suggestive of substantial electron density on the ligand, supporting the assignment of the first electrochemical reduction as being ligand based.[50]

Dianionic species **6** was formed by the addition of 2.2 equivalents of KC_8 to a THF solution of **4** in the presence of 18-crown-6. The ^{1}H NMR spectrum of the black-purple solution of complex **6** in THF-d_8 (Fig. S9†) showed signals for a diamagnetic compound, with bipyridine ligands that were significantly shifted upfield from the starting material (4.80, 6.60, and 8.47 ppm for **6** *vs.* 7.58, 8.40, and 9.10 ppm for **4**). This upfield shift in the C–H protons on the bipyridine ligand has also been observed in the $[Al(bpy\text{-}H)_2]^-$ anion, which has been assigned as possessing two $(bpy\text{-}H)^{2-}$ ligands.[51]

A diffracting crystal of **6** was obtained after multiple crystallization attempts. Although several issues exist with the structure, it was found to be the $[W(bpy\text{-}t\text{Bu})(CO)_3][K(18\text{-crown-}6)]_2$ species. The dianion crystallizes between two layers of the 18-crown-6 ligands, which display significant disorder (Fig. S7 in the ESI†). The C9–C10 distance in **6** is significantly shorter than the corresponding bond in **4** (1.483 Å). The C–O distances in the carbonyl ligands of **6** are also significantly longer than those in **4**.

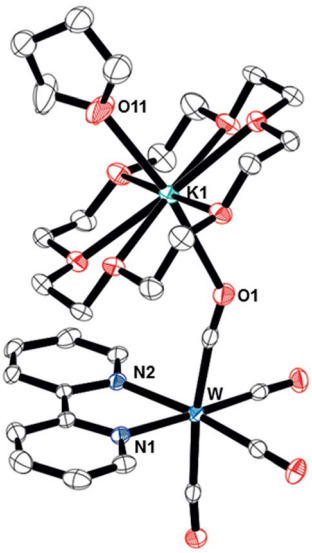

Fig. 4 Molecular structure of $[W(bpy)(CO)_4][K(18\text{-crown-}6)\cdot THF]$ (**5**). Ellipsoids are shown at 50% probability. Hydrogen atoms are omitted for clarity.

The lengthening of the metal–carbonyl bonds in **5** and **6** due to the increased back bonding from the metal is consistent with the FT-IR spectra of these complexes. The carbonyl stretching frequencies of complex **4** shift to a lower frequency by roughly 30 cm^{-1} upon the first chemical reduction, and the subsequent reduction leads to the dianion **6**, which exhibits a band at 1837 cm^{-1} and a broad band at 1713 cm^{-1} as shown in Fig. 5 (the IR spectra of **5** and of the dianion $[W(bpy)(CO)_3]^{2-}$ are shown in Fig. S8 in the ESI†). These ν(CO) bands are observed at much lower frequencies than $[Re(bpy\text{-}t\text{Bu})(CO)_3]^-$ (1940 cm^{-1} and 1835 cm^{-1}) and $Mn(bpy\text{-}t\text{Bu})(CO)_3]^-$ (1911 cm^{-1} and 1813 cm^{-1}) anions that are isoelectronic with **6**. This indicates that

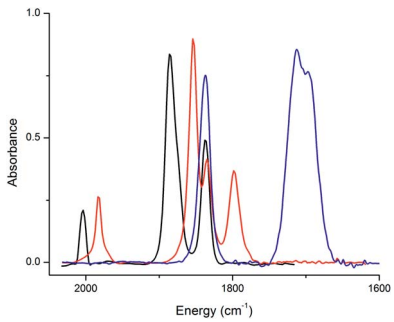

Fig. 5 FT-IR spectra of the chemically reduced species of W(bpy-*t*Bu)$(CO)_4$ (**4**) in THF under N_2. The neutral species **4** (black) has ν(CO) stretches of 2004 cm^{-1}, 1886 cm^{-1}, and 1837 cm^{-1}. The chemically reduced anion (red) ν(CO) stretches are 1982 cm^{-1}, 1854 cm^{-1}, 1835 cm^{-1}, and 1798 cm^{-1}; the doubly reduced species **6** (blue) ν(CO) stretches are 1837 cm^{-1} and 1713 cm^{-1}.

the anion **6** has much stronger back donation to the antibonding π* orbitals of the CO ligands than the corresponding Re or Mn monoanions with the same ligand sets.

DFT calculations of catalytically relevant complexes

In order to obtain a deeper insight into the species formed upon electrochemical reduction of **4**, the DFT-optimized structures of the reduced species obtained from **4** were calculated. Geometry optimized structures were obtained by using the X-ray coordinates of **4** and **6** as the initial inputs to obtain the structures of the neutral form (**A**) and the five-coordinate dianion (**D**). The geometry of the mono-reduced species $[W(bpy\text{-}tBu)(CO)_4]^{-1}$ (**B**) and the doubly-reduced species structure $[W(bpy\text{-}tBu)(CO)_4]^{-2}$ (**C**) were then optimized from **A** (Scheme 2). Frequency calculations were used to establish that the optimized structures were not transition states. The crystal structure for **6** and the DFT-optimized structure of **D** are intermediate between a square pyramid and a trigonal bipyramid ($\tau_5 = 0.44$ and 0.46, respectively)[52] (Fig. 6). Pertinent bond distances for the calculated structures and coordinates for the optimized structures are included in the ESI.† The calculated ν(CO) stretching frequencies for species **D** (1822, 1734, and 1724 cm^{-1}) agree well with the ν(CO) band energies observed in IR for the reduced species **6** in THF (1837 cm^{-1} and a broad band at 1713 cm^{-1}). A comparison of the calculated and experimental ν(CO) stretching frequencies for species **A–D** is included in the ESI (Table S5).† The central C–C bonds in the bipyridine ligands in the dianions **C** and **D** are significantly shortened compared to **A** and **B**, with C–C bond lengths of 1.390 and 1.398 Å for the central C–C bond in the bipyridine ligand in the octahedral (**C**) and five-coordinate (**D**) complexes. The bond lengths for **C** and **D** are shorter than the bond lengths in the neutral complex (1.463 and 1.481 Å for geometry optimization (**A**) and X-ray structure of **4**), and the monoanion (**B**) (1.423 Å). These results are consistent with our understanding of the system from the electrochemical and structural studies, indicating that the bipyridine accepts a significant amount of the electron density from both $1e^-$ reductions observed in the electrochemistry of **1–4**.

Examination of the calculated highest occupied molecular orbitals (HOMOs) and lowest unoccupied molecular orbitals (LUMOs) of complexes **A–D** provides further insights about these complexes. The calculated HOMO of the dianion **D** is delocalized over the bipyridine and somewhat over the tungsten center (Fig. 6). In comparison, the LUMO, singly occupied molecular orbital (SOMO) and HOMO of **A**, **B**, and **C** are primarily localized on the bipyridine with some electron density on the CO ligands (see ESI†). The calculated HOMO for species **D** is qualitatively similar to the calculated HOMO for the $[Re(bpy\text{-}tBu)(CO)_3]^{-1}$ anion, which is the reactive species in catalysis with $Re(bpy\text{-}tBu)(CO)_3X$ catalysts.[8] Calculations on a related species, $[Mn(bpy\text{-}H)(CO)_3]^{-1}$ also showed that the HOMO of this species is delocalized over the bipyridine ligand as well as the metal center.[53]

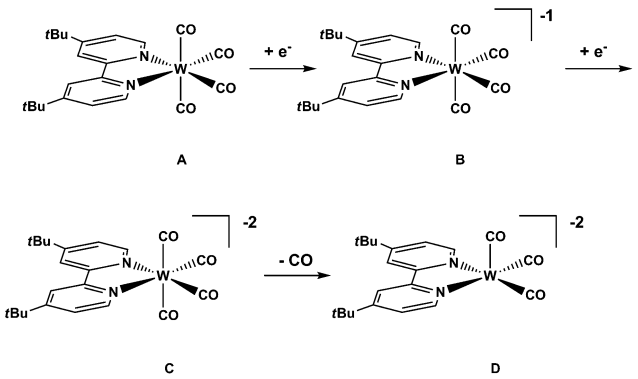

Scheme 2 Complexes based on complex **4** that were studied using DFT calculations.

Comparison with group 7 catalysts

A comparison of the catalytic activities of **1–4** with analogous group 7 complexes is shown in Table 2. The group 6 species are similar in activity to $[Re(bpy\text{-}tBu)(CO)_3(CH_3CN)](OTf)$ and more active than the corresponding Mn species under the same conditions (Mn complexes do not exhibit catalysis without added protons). Upon the addition of a proton source, the group 7 catalysts greatly outperform the W and Mo species. The effect of adding a Brönsted acid could not be quantified for the group 6 species due to the negative potentials of the second reductions being too close to the direct reduction of the acids at the electrodes in the cyclic voltammetry experiments.

While the Mo and W complexes reported herein are not exceptional electrocatalysts for CO_2 reduction, their study is very valuable because it provides a framework in which to understand similar electrocatalysts, such as the group 7 species. Through comparisons of the structurally similar and isoelectronic group 6 $M(bpy\text{-}R)(CO)_4$ species and the group 7 $M(bpy\text{-}R)(CO)_3X$ species, we can understand what characteristics lead to efficient and active catalysts.

The first electrochemical reduction of both the group 6 (**1–4**) and group 7 $M(bpy\text{-}R)(CO)_3X$ (M = Re, Mn) electrocatalysts proceeds through reduction of the bipyridine ligand. In the

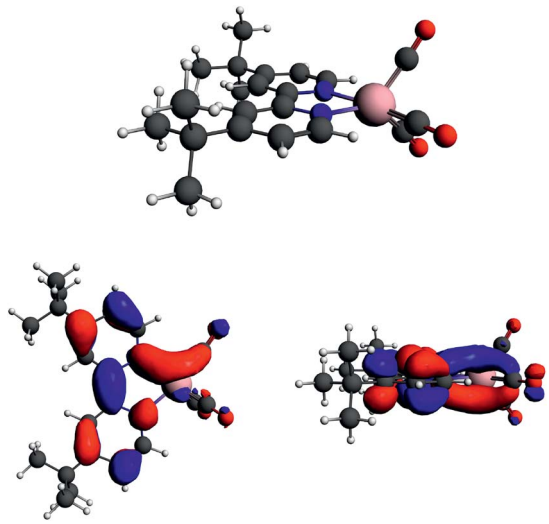

Fig. 6 Ball and stick representation of the geometry optimized structure (top) and the DFT-calculated HOMO (bottom left: top view; right: side view) of the five-coordinate dianionic species **D**.

rhenium system, ligand loss (dissociation of the chloride or other X ligand) subsequently occurs from $[Re(bpy\text{-}R)(CO)_3X]^-$ leading to a species that can be assigned as a Re(0) center and a neutral bipyridine ligand. Ultimately, a Re(0)–Re(0) dimer is formed, and characterization of the dimer gives clear indication that the reduction has occurred at the metal center.[54] For manganese, reduction of a $Mn(bpy\text{-}R)(CO)_3X$ species leads to extremely rapid dimerization such that monomeric $[Mn(bpy\text{-}R)(CO)_3X]^-$ species have not been observed spectroscopically. In stark comparison, the group 6 complexes do not lose a ligand or dimerize upon reduction, but rather the axial carbonyl becomes somewhat more susceptible to substitution.[43] However, the electron density remains primarily over the bipyridine ligand, and the carbonyl ligand remains strongly coordinated enough that we were able to crystallize the $[W(bpy)(CO)_4]^-$ anion (complex **5**), wherein the bipyridine ligand is clearly reduced. Notably, reduction of a $[Re(bpy\text{-}R)(CO)_4]^+$ cation does not lead to an observable $Re(bpy\text{-}R)(CO)_4$ species,[42] indicating that the group 6 complexes bind CO more strongly than the group 7 complexes.

A second reduction in both the group 6 and the group 7 systems leads to a diamagnetic complex with five-coordinate geometry and a similar HOMO delocalized over the metal and the bipyridine. For the rhenium complexes, XANES data suggests that these species are best described as $M^0(bpy^{-1})$. The second reduction in the $Re(bpy\text{-}R)(CO)_3Cl$ systems is 300–400 mV more negative than the first, however the second reduction potentials of **1–4** are 540–590 mV more negative than their first reduction. This is similar to the separation observed between the 2,2′-bipyridine monoanion and dianion.[55] Thus it seems reasonable that they are described as $M^0(bpy^{-2})$ species, rather than $M^{-1}(bpy^{-1})$ or $M^{-2}(bpy^0)$ complexes. Further studies are needed to unambiguously assign these ground states.

These comparisons lead to two important conclusions about electrocatalysts for CO_2 reduction. The first is that having catalytically relevant electrons stored in both the bipyridine ligand and the metal center leads to a lower overpotential compared to having two electrons stored on the bipyridine ligand. The second conclusion about these electrocatalysts is that having a complex that strongly back-donates to CO is undesirable because it will hinder release of the product and slow overall catalysis, *i.e.* CO poisoning of the catalyst.

Conclusions

Electrochemical experiments on groups 6 complexes **1–4** $M(bpy\text{-}R)(CO)_4$ (R = H, M = Mo (**1**), W (**2**); R = *t*Bu, M = Mo (**3**), W (**4**)) have shown that these complexes are competent catalysts for CO_2 reduction through a two-electron reduction process to generate a diamagnetic dianionic complex. The reduced species have been studied using X-ray crystallography, IR spectroscopy and DFT calculations. These catalysts display stronger back donation to CO than group 7 catalysts, which may explain why they operate at slower rates. Future studies will include studying the stoichiometric reactions of the reduced species with CO_2 and H^+ sources, as well as attempting to elucidate the full catalytic cycle. The catalytic cycle of CO_2 reduction by $Re(bpy)(CO)_3Cl$ has recently been elucidated by computational methods, and similar study of group 6 catalysts would be very informative.[56] Complexes **1–4** are rare examples of group 6 electrocatalysts for CO_2 reduction and future work will focus on developing more efficient and selective catalysts based on these relatively abundant metals.

Acknowledgements

This material is based upon work supported by the Air Force Office of Scientific Research through the MURI program under AFOSR Award No. FA9550-10-1-0572. Dr. Jonathan M. Smieja, Dr. Eric E. Benson, Jesse Froehlich, and Matthew Sampson are acknowledged for valuable discussions and assistance with electrochemistry, chemical reductions, and crystallography. Professor Joshua Figueroa, Professor John A. Keith, Steve George, and Alissa Sasayama are acknowledged for assistance with DFT calculations.

Notes and references

1 E. E. Benson, C. P. Kubiak, A. J. Sathrum and J. M. Smieja, *Chem. Soc. Rev.*, 2009, **38**, 89–99.
2 J.-M. Savéant, *Chem. Rev.*, 2008, **108**, 2348–2378.
3 C. D. Windle and R. N. Perutz, *Coord. Chem. Rev.*, 2012, **256**, 2562–2570.
4 C. Costentin, M. Robert and J.-M. Saveant, *Chem. Soc. Rev.*, 2013, **42**, 2423–2436.
5 A. M. Appel, J. E. Bercaw, A. B. Bocarsly, H. Dobbek, D. L. DuBois, M. Dupuis, J. G. Ferry, E. Fujita, R. Hille, P. J. A. Kenis, C. A. Kerfeld, R. H. Morris, C. H. F. Peden, A. R. Portis, S. W. Ragsdale, T. B. Rauchfuss, J. N. H. Reek, L. C. Seefeldt, R. K. Thauer and G. L. Waldrop, *Chem. Rev.*, 2013, **113**, 6621–6658.
6 J. Hawecker, J. M. Lehn and R. Ziessel, *J. Chem. Soc., Chem. Commun.*, 1984, 328–330.
7 J. M. Smieja and C. P. Kubiak, *Inorg. Chem.*, 2010, **49**, 9283–9289.
8 J. M. Smieja, E. E. Benson, B. Kumar, K. A. Grice, C. S. Seu, A. J. Miller, J. M. Mayer and C. P. Kubiak, *Proc. Natl. Acad. Sci. U. S. A.*, 2012, **109**, 15646–15650.
9 K. A. Grice and C. P. Kubiak, *Adv. Inorg. Chem.*, eds. M. Aresta and R. van Eldik, Academic Press, 2014, **66**, 163–188.
10 M. Bourrez, F. Molton, S. Chardon-Noblat and A. Deronzier, *Angew. Chem., Int. Ed.*, 2011, **50**, 9903–9906.
11 J. M. Smieja, M. D. Sampson, K. A. Grice, E. E. Benson, J. D. Froehlich and C. P. Kubiak, *Inorg. Chem.*, 2013, **52**, 2484–2491.
12 J. D. Froehlich and C. P. Kubiak, *Inorg. Chem.*, 2012, **51**, 3932–3934.
13 I. Bhugun, D. Lexa and J.-M. Savéant, *J. Phys. Chem.*, 1996, **100**, 19981–19985.
14 C. Costentin, S. Drouet, M. Robert and J.-M. Savéant, *Science*, 2012, **338**, 90–94.
15 A. M. Lilio, K. A. Grice and C. P. Kubiak, *Eur. J. Inorg. Chem.*, 2013, **2013**, 4016–4023.
16 J. A. Ramos Sende, C. R. Arana, L. Hernandez, K. T. Potts, M. Keshevarz-K and H. D. Abruna, *Inorg. Chem.*, 1995, **34**, 3339–3348.

17 C. J. Pickett and D. Pletcher, *J. Chem. Soc., Dalton Trans.*, 1976, 749–752.
18 T. Reda, C. M. Plugge, N. J. Abram and J. Hirst, *Proc. Natl. Acad. Sci. U. S. A.*, 2008, **105**, 10654–10658.
19 H. Dobbek, L. Gremer, R. Kiefersauer, R. Huber and O. Meyer, *Proc. Natl. Acad. Sci. U. S. A.*, 2002, **99**, 15971–15976.
20 G. R. Lee, J. M. Maher and N. J. Cooper, *J. Am. Chem. Soc.*, 1987, **109**, 2956–2962.
21 U. Jayarathne, P. Chandrasekaran, H. Jacobsen, J. T. Mague and J. P. Donahue, *Dalton Trans.*, 2010, **39**, 9662–9671.
22 L. Contreras, M. Paneque, M. Sellin, E. Carmona, P. J. Perez, E. Gutierrez-Puebla, A. Monge and C. Ruiz, *New J. Chem.*, 2005, **29**, 109–115.
23 B. L. Yonke, J. P. Reeds, P. Y. Zavalij and L. R. Sita, *Angew. Chem., Int. Ed.*, 2011, **50**, 12342–12346.
24 W. H. Bernskoetter and B. T. Tyler, *Organometallics*, 2011, **30**, 520–527.
25 C.-C. Tai, T. Chang, B. Roller and P. G. Jessop, *Inorg. Chem.*, 2003, **42**, 7340–7341.
26 D. J. Darensbourg and C. Ovalles, *J. Am. Chem. Soc.*, 1984, **106**, 3750–3754.
27 A. Vlček Jr, *Coord. Chem. Rev.*, 2002, **230**, 225–242.
28 Y. Kaizu and H. Kobayashi, *Bull. Chem. Soc. Jpn.*, 1972, **45**, 470–477.
29 T. S. A. Hor and S.-M. Chee, *J. Organomet. Chem.*, 1987, **331**, 23–28.
30 E. Tolun, C. J. Proctor, J. F. J. Todd, J. M. A. Walshe and J. A. Connor, *Org. Mass Spectrom.*, 1984, **19**, 294.
31 M. J. Schadt and A. J. Lees, *Inorg. Chem.*, 1986, **25**, 672–677.
32 S. Cao, K. Bal Reddy, E. M. Eyring and R. van Eldik, *Organometallics*, 1994, **13**, 91–93.
33 J. A. Connor and C. Overton, *J. Organomet. Chem.*, 1983, **249**, 165–174.
34 R. Johnson, H. Madhani and J. P. Bullock, *Inorg. Chim. Acta*, 2007, **360**, 3414–3423.
35 S. S. Braga, A. C. Coelho, I. S. Gonçalves and F. A. Almeida Paz, *Acta Crystallogr., Sect. E: Struct. Rep. Online*, 2007, **63**, m780–m782.
36 Q. Ye, Q. Wu, H. Zhao, Y.-M. Song, X. Xue, R.-G. Xiong, S.-M. Pang and G.-H. Lee, *J. Organomet. Chem.*, 2005, **690**, 286–290.
37 J. Chapman, G. Kolawole, N. Long, A. J. P. White, D. J. Williams and P. O'Brien, *S. Afr. J. Sci.*, 2005, **101**, 454–456.
38 C. C. Scarborough and K. Wieghardt, *Inorg. Chem.*, 2011, **50**, 9773–9793.
39 F. Allen, *Acta Crystallogr., Sect. B: Struct. Sci.*, 2002, **58**, 380–388.
40 C. Makedonas and C. A. Mitsopoulou, *Eur. J. Inorg. Chem.*, 2007, **2007**, 110–119.
41 T. Scheiring, W. Kaim and J. Fiedler, *J. Organomet. Chem.*, 2000, **598**, 136–141.
42 K. A. Grice, N. X. Gu, M. D. Sampson and C. P. Kubiak, *Dalton Trans.*, 2013, **42**, 8498–8503.
43 D. Miholová and A. A. Vlček, *J. Organomet. Chem.*, 1985, **279**, 317–326.
44 D. Miholová, B. Gaš, S. Záliš, J. Klíma and A. A. Vlček, *J. Organomet. Chem.*, 1987, **330**, 75–84.
45 R. J. Crutchley and A. B. P. Lever, *Inorg. Chem.*, 1982, **21**, 2276–2282.
46 R. E. Dessy and L. Wieczorek, *J. Am. Chem. Soc.*, 1969, **91**, 4963–4974.
47 R. E. Dessy, F. E. Stary, R. B. King and M. Waldrop, *J. Am. Chem. Soc.*, 1966, **88**, 471–476.
48 J. A. Connor, C. Overton and N. El Murr, *J. Organomet. Chem.*, 1984, **277**, 277–284.
49 J. A. Vlček, F. Baumann, W. Kaim, F.-W. Grevels and F. Hartl, *J. Chem. Soc., Dalton Trans.*, 1998, 215–220.
50 E. Gore-Randall, M. Irwin, M. S. Denning and J. M. Goicoechea, *Inorg. Chem.*, 2009, **48**, 8304.
51 G. B. Nikiforov, H. W. Roesky, M. Noltemeyer and H. G. Schmidt, *Polyhedron*, 2004, **23**, 561.
52 A. W. Addison, T. N. Rao, J. Reedijk, J. van Rijn and G. C. Verschoor, *J. Chem. Soc., Dalton Trans.*, 1984, 1349–1356.
53 F. Hartl, P. Rosa, L. Ricard, P. Le Floch and S. Záliš, *Coord. Chem. Rev.*, 2007, **251**, 557–576.
54 E. E. Benson and C. P. Kubiak, *Chem. Commun.*, 2012, **48**, 7374–7376.
55 M. Krejčik and A. A. Viček, *J. Electroanal. Chem. Interfacial Electrochem.*, 1991, **313**, 243–257.
56 J. A. Keith, K. A. Grice, C. P. Kubiak and E. A. Carter, *J. Am. Chem. Soc.*, 2013, **135**, 15823–15829.

